Joint Analysis of Personalized In-Silico Haemodynamics and Shape Descriptors of the Left Atrial Appendage

Jordi Mill[1], Andy L. Olivares[1], Etelvino Silva[2], Ibai Genua[1], Alvaro Fernandez[1], Ainhoa Aguado[1], Marta Nuñez-Garcia[1], Tom de Potter[2], Xavier Freixa[3], and Oscar Camara[1(✉)]

[1] DTIC (Department of Information and Communication Technologies), Universitat Pompeu Fabra, Barcelona, Spain
oscar.camara@upf.edu
[2] Arrhythmia Unit, Department of Cardiology, Cardiovascular Center, OLV Hospital, Aalst, Belgium
[3] Department of Cardiology, Hospital Clinic de Barcelona, Universitat de Barcelona, Barcelona, Spain

Abstract. The left atrial appendage (LAA) is a complex and heterogeneous bulge structure of the left atrium (LA). It is known that, in atrial fibrillation (AF) patients, around 70% to 90% of the thrombi are formed there. However, the exact mechanism of the process of thrombus formation and the role of the LAA in that process are not fully understood yet. The main goal of this work is to perform patient-specific haemodynamics simulations of the LA and LAA and jointly analyse the resulting blood flow parameters with morphological descriptors of these structures in relation with the risk of thrombus formation. Some LAA morphological descriptors such as ostium characteristics and pulmonary configuration were found to influence LAA blood flow patterns. These findings improve our knowledge on the required conditions for thrombus formation in the LAA.

Keywords: Computational fluid dynamics · Left atrial appendage · Blood flow patterns · Thrombus formation

1 Introduction

Atrial fibrillation (AF) is an arrhythmia produced by a re-entry and/or rapid focal ectopic firing that affects 1 to 2% of the population, and about 8% of the individuals over 80 years of age [1]. It is known that AF is the most common cardiac abnormality associated with ischemic strokes [2]. Chronic atrial fibrillation causes rigidity on left atrial (LA) walls, preventing its proper contraction and altering the normal left atrial haemodynamics. This scenario could lead to blood stagnation in the left atrial appendage (LAA), increasing the risk of thrombus formation [3]. In fact, 25% of embolic strokes are due to AF, mainly caused by the formation of thrombus; a high percentage, around 70% to 90%, of thrombi occurring during AF derive from the LAA [4]. The LAA is a little portion of cardiac anatomy structure that develops during the third week of gestation. It has a wide shape spectrum among individuals and its

M. Pop et al. (Eds.): STACOM 2018, LNCS 11395, pp. 58–66, 2019.
https://doi.org/10.1007/978-3-030-12029-0_7

classification depends on the number of lobes, the length or the angle between the LAA and its ostium. If the thrombus leaves the LAA and is released onto the circulatory system, it can travel to the brain and cause an embolic stroke.

Despite of the high incidence of embolic strokes on AF patients and the known role of the LAA, the relationship among LA, LAA and thrombus is not clear yet. The exact dependence between morphological parameters and LA haemodynamics on patient-specific geometries needs to be established. Recent studies claimed that some LAA morphologies (e.g. non chicken-wing) were more likely to produce thrombi [5]. Others used indices such as the ostium diameter, the number of lobes or other anatomical parameters that are difficult to reproduce or reach a consensus [4, 6]. The influence of the haemodynamics stimuli in the LAA on the thrombi formation process has been studied by many researchers [7]. Low flow velocities in the LAA are associated with a higher risk of stroke among AF patients. However, the flow is assessed from Trans-esophageal Echocardiographic (TEE) images, only providing partial flow data on a plane or a given point of view, which is insufficient. Novel technics such as 3D echography and 4D PC-MRI can provide information in terms of blood velocity and thrombus localization, but not all the hospitals have access to these and their resolution is not good enough to produce a subsequent quantitative haemodynamic analysis such as the presented in this manuscript.

Considerable progress has been achieved on the development of computational technologies and computational fluid dynamics (CFD) methods. Such methods allow the application of image-based CFD simulations to understand the effects of haemodynamics in vascular pathologies and its pathophysiology, which is known to be related with thrombus formation [8]. Some researchers have already used CFD to study the LAA, assessing 3D blood flow patterns in different LA/LAA configurations [9–11]. However, these studies either used synthetic models or not jointly analyzing blood flow simulations with morphological descriptors.

The main goal of this work was to perform a joint analysis of morphological and in silico haemodynamics descriptors on clinical data from four AF patients. Blood flow simulations were personalized with patient-specific pressure data and validated with Doppler ultrasound images.

2 Material and Methods

2.1 Patient Data and Model Reconstruction

Imaging data from four patients was processed in this work to build the anatomical reference for the simulations: three 3D Rotational Angiography (3DRA) images were provided by OLV Hospital, Aalst, Belgium; the fourth dataset was a Computational Tomography (CT) scan from Hospital Clinic de Barcelona, Spain. The data was anonymized and a written consent was obtained from all patients. Regarding patients from Belgium, the following data were also provided: the pressure in the mitral valve, the atrium, the pulmonary veins and in the LAA. This anonymous information is valuable because it provides data for validation and verification. Moreover, full echocardiography datasets including multiple chamber views and Doppler acquisitions were provided for all cases.

The anatomical structure of the left atrium was semi-automatically extracted from each medical image using Seg3D: Volumetric Image Segmentation and Visualization[1]. The output segmentation was transformed into a surface mesh of triangular elements with the classical Marching Cubes algorithm. Subsequently, a Taubin filter with the threshold set to 0.7 was applied to smooth the surface mesh using Meshlab[2].

Due to the surgery and data acquisition process, a catheter was needed during the intervention, which appears in the 3DRA images. Furthermore, the direction and shape of the veins were too irregular from the segmentations. In addition, the resolution was still too low to allow a good jet flow development in the simulations as well as to extract the cardiac valve accurately enough (mitral valve in the case of the left atria). For all the reasons mentioned above, the surface mesh was refined using Meshlab and MeshMixer[3], as can be seen in Fig. 1. The next step was to generate a tetrahedral volumetric mesh from the surface mesh, which was obtained with Gmsh[4].

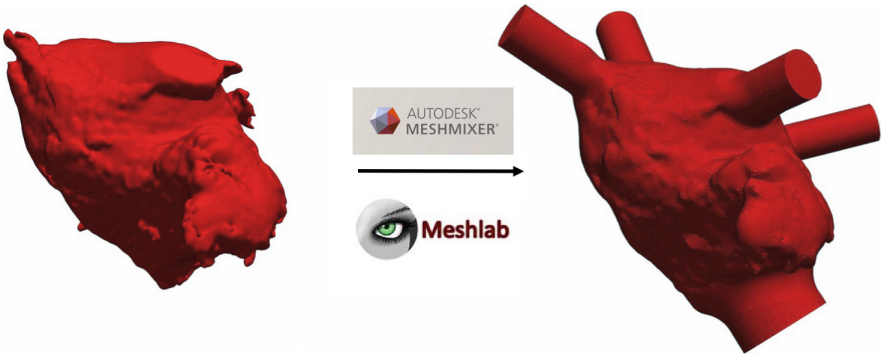

Fig. 1. An example of computational mesh building from patient-specific geometries (Patient 1).

2.2 Computational Fluid Dynamics Model

For the four processed cases a second order implicit unsteady formulation was used for the solution of the momentum equations in conjunction with a standard partial discretization for the pressure (under-relaxation factors set by default to 0.3 and 0.7 for the pressure and momentum, respectively). The equations were solved using finite volume method (FVM) in Ansys Fluent 18.2 (academic research CFD solver)[5]. Blood flow in the LA was modeled using the incompressible Navier Stokes and continuity equations. Absolute residuals of mass and momentum conservation equations lower than 0.005

[1] http://www.seg3d.org.
[2] http://www.meshlab.net/.
[3] http://www.meshmixer.com.
[4] http://gmsh.info/.
[5] https://www.ansys.com/products/fluids/ansys-fluent.

were absolute convergence criteria. Blood was modeled as an incompressible Newtonian fluid with a density value of 1060 kg/m^3 [10]. The dynamic viscosity of blood in large vessels and the heart was set to 0.0035 Pa · s [10]. Simulations were run using a laminar flow hypothesis under isothermal and no-gravitational effects. All walls were simulated rigid and with no-slip conditions and therefore replicating the arguably worst-case scenario in AF, without atrial contraction.

The differential equations were solved using a time-step of 0.01 s during one beat, that means 105 steps overall, where the ventricular systole phase lasts 0.4 s and the ventricular diastole lasts 0.65 s. Following the clinical observations of Fernandez-Perez et al. [12] an equal time-velocity function was applied at the four pulmonary veins for all the four patients. At the mitral valve a pressure of 8 mmHg was imposed during the ventricular diastolic phase. In ventricular systole, the MV is closed and was simulated as a wall boundary. Subsequently, the model of each case was imported to Ansys Fluent.

2.3 Morphological and Haemodynamics Descriptors

The morphological indices, extracted using MATLAB R2017b (Mathworks, MS, USA)[6] were the following: (1) mean ostium diameter, being the average between the maximum and minimum diameter; (2) ostium maximum diameter; (3) ostium perimeter; (4) ostium area; (5) volume of the LAA; and (6) the centreline length, being the distance between the centre of the ostium and the furthest point of the anatomy using a heat equation. Therefore, a gradual distribution is obtained and to find the farthest point of the geometry. From that point, the other points can be calculated using a marching algorithm and generating the centerline.

Flow simulations were assessed at the pulmonary veins (PV), mitral valve (MV), the middle of the left atrium and the LAA. Furthermore, wall shear stress (WSS), defined as the frictional force exerted by the flowing blood tangentially to the wall, was also estimated from the flow simulations. This parameter has been strongly associated with endothelial lesions and thrombus formation [13]. From the WSS, some parameters that have also been related to the risk of thrombus formation were calculated: Time Averaged Wall Shear Stress (TAWSS), the Oscillatory Shear Index (OSI), the Endothelial Cell Activation Potential (ECAP). Theoretically, regions with low TAWSS and high OSI are more prone to develop atherosclerosis [6]. In an attempt to localize these regions, Di Achille et al. [14] proposed using the ratio of these two indices to characterize the degree of susceptibility of the area to generate a thrombus, also known as ECAP. Whether the ECAP values are high, then that area has more potential to be susceptible to generate a thrombus.

[6] https://es.mathworks.com/products/matlab.html.

3 Results

This work has presented a methodology to assess the probability to generate a thrombus at LAA in a non-invasive and patient-specific manner from medical images and computational simulations. In order to validate this workflow and its results, personalized data for each patient such as ultrasound images and pressure profiles were collected. According to literature, patients with atrial fibrillation do not have the A curve that can be seen in healthy patients [15]. Figure 2(a) and (c) displays the Doppler ultrasound image from Patient 4 and its respective blood flow simulation at the MV. As shown, there is no A wave in both, simulation and ultrasound imaging, only the E wave is present.

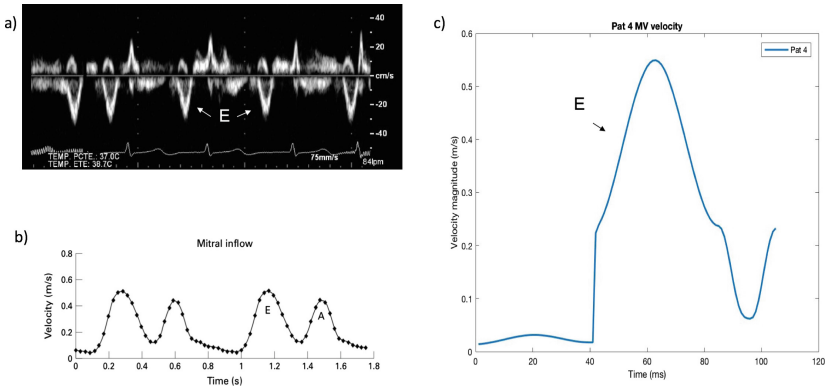

Fig. 2. (a) Doppler ultrasound image from Patient 4; (b) Mitral Valve (MV) velocity curve from the literature [15]; (c) Mitral valve velocity curve from our blood flow simulations.

3.1 Morphological Descriptors

The morphological parameters from the LAA of the four patients under study are displayed in Table 1. The results among the four patients are relatively similar except Patient 4, who seems to have a larger LAA. However, the longest centreline length corresponds to Patient 1 since it has more secondary lobes and bulges than Patient 4

Table 1. Morphological parameters for each LAA

	Mean diam. (mm)	Max. diam. (mm)	Ostium perimeter (mm)	Ostium area (mm^2)	LAA volume (mL)	LA volume (mL)	Centreline length (mm)
Patient 1	22.53	26.58	72.07	384.93	6.86	188.51	42.76
Patient 2	23.08	26.40	76.26	422.95	6.06	181.07	27.56
Patient 3	25.97	32.56	82.40	499.63	7.02	137.59	31.16
Patient 4	31.45	35.43	97.40	762.00	10.16	303.56	30.11

(see Fig. 3). As has been mentioned previously, these parameters are related with the risk of thrombus formation [10, 16]. The higher are these morphological values, the higher is the probability to generate a thrombus. Therefore, Patient 1 and Patient 4 would be the ones with more risk according to the morphological parameters.

3.2 Haemodynamic Descriptors

Streamlines are used to visualize which flow trajectories are following the particles and, in our study, if these are going into the LAA. It can also help to find the origin of these particles and figure out which pulmonary veins contribute to flow entering the LAA, depending on PV number, orientation and spatial distribution. Figure 3 shows the same time step from diastole in all cases. The left superior pulmonary vein always provides blood flow to the LAA. This makes sense since it is the closest to the LAA; in some cases, just below it. However, the other PV that provide flow to the LAA vary

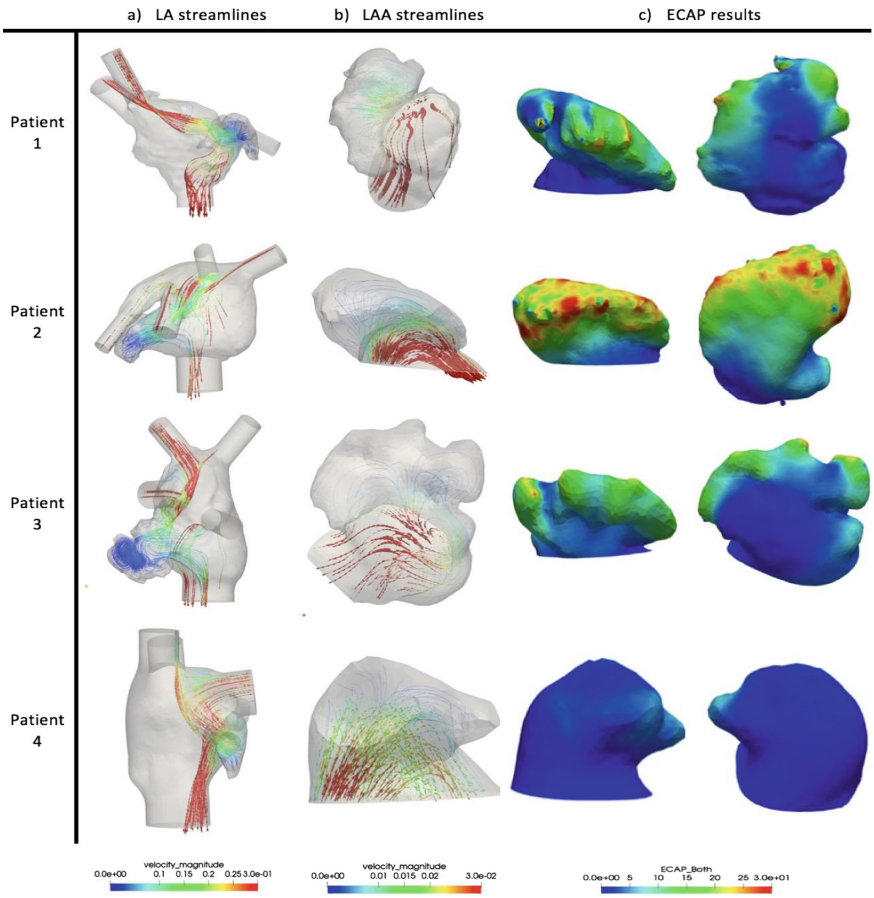

Fig. 3. (a) Streamlines of blood flow in the left atria entering the left atrial appendage at second 0.6 (diastole); (b) Flow streamlines in the LAA; (c), (d) frontal and posterior views, respectively, of Endothelial Cell Activation Potential (ECAP) maps in the LAA.

depending on their orientation, without a common pattern among the studied patients. Moreover, the combination of both, the PV configuration and LAA morphology, especially ostium characteristics, determines the amount of flow reaching the distant parts of the LAA (see Fig. 3).

The ECAP results presented in Fig. 3 show that Patient 4 had the lowest ECAP values, although it had a high probability of developing thrombus according to the morphological parameters. On the other hand, Patient 1 and 3 reached high ECAP values on some secondary lobes. Patient 2 presented a high probability to generate thrombi in almost all the parts of its LAA. Nevertheless, Patient 2 ECAP values could be explained by the lack of flow entering the LAA over the whole the cardiac cycle, especially during the systole. If velocity values inside the LAA are very low, large values of ECAP are reached.

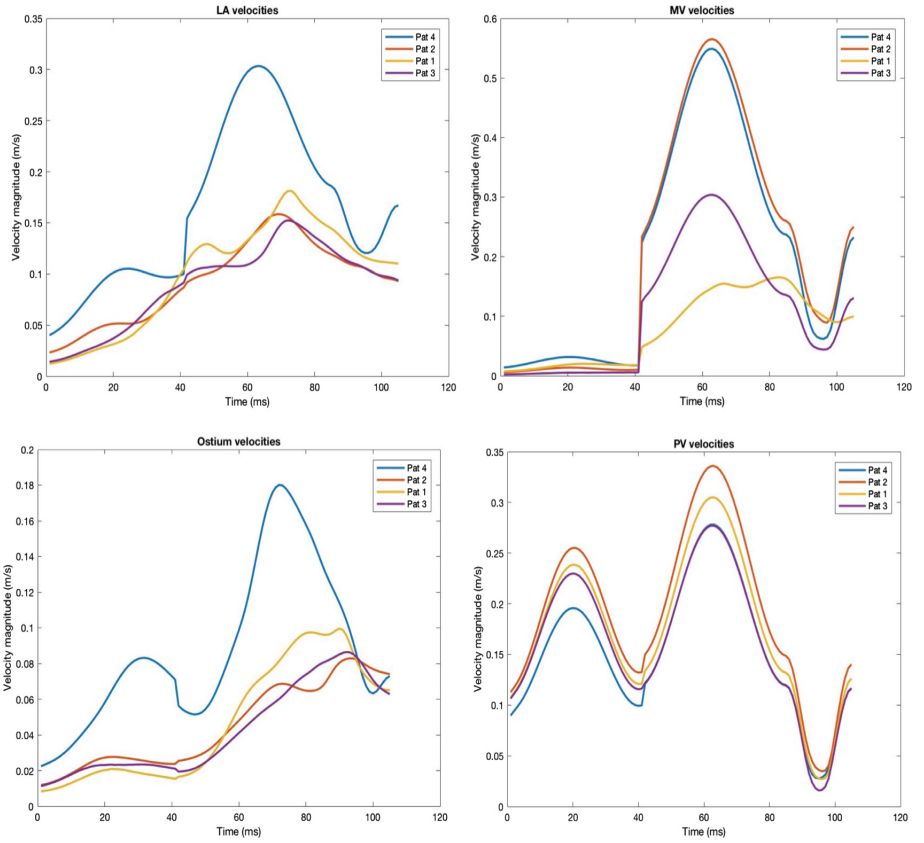

Fig. 4. Comparison of the velocity magnitude among the cases with LAA in the different sampling areas (PV, MV, Ostium, LA).

For all the patients, a velocity average at different parts of the left atrium was carried out: (1) at the middle of the LA; (2) at the MV; (3) at the end of the LSPV and LAA's ostium (see Fig. 4). From 0 ms to 40 ms corresponds to systole phase, and from 60 ms to 105 ms the diastole. Since during the systole the MV is closed, the velocities are lower at the beginning of the cycle and at the MV are almost zero.

4 Conclusions

There are studies aimed at determining the probability to generate thrombi solely based on morphological parameters of the LAA [16]. Such an approach simplifies the study excessively, in particular due to the absence of robust ways to fully characterize LAA morphology [17]. The work described in this manuscript presents a workflow to assess patient haemodynamics in the LA/LAA and its risk to develop thrombi with blood flow simulations, which provide complementary information to morphological parameters.

The four studied patients had similar morphological parameters but their ECAP distribution were very different. Furthermore, Patient 4, being the one with the highest probability of developing thrombi according to morphological parameters (maximum ostium diameter and larger volume), was the one with the lowest ECAP. However, these differences might be due to the different imaging system used in Patient 4 with respect to the other patients. On the other hand, Patient 2 presented the highest likelihood to produce thrombi according to ECAP distribution, likely due to the low blood flow velocities entering the LAA during systole.

Overall, differences in ECAP distribution in the analyzed patients should be related to their LA/LAA anatomies since boundary conditions were the same in the simulations. Therefore, it is clear that LAA morphological parameters play a critical role in thrombus formation but other factors need to be considered. For instance, we have observed that LAA flow is highly dependent on how PV are localized in the LA, allowing to produce complex flow patterns in the cavity. In consequence, both morphological and haemodynamics parameters should be jointly analyzed for a more complete understanding of the mechanisms inducing thrombus formation. Future work would focus on running the whole modelling pipeline in a large number of cases and perform advanced statistical studies to identify which parameters are different in AF patients with and without a history of thromboembolic events.

Acknowledgments. This work was partially supported by COMPILAAO Retos I+D project (DPI2015-71640-R), funded by the Spanish Government of Economy and Competitiveness.

References

1. Pellman, J., Sheikh, F., Diego, S., Jolla, L.: Atrial fibrillation: mechanisms, therapeutics, and future directions. Compr. Physiol. **5**(2), 649–665 (2017)
2. Chugh, S.S., Havmoeller, R., Narayanan, K., Kim, Y., McAnulty Jr., J.H.M., Zheng, Z.: Worldwide epidemiology of atrial fibrillation: a global burden of disease 2010 study. Circulation **129**(8), 837–847 (2014)

3. Fatkin, D., Kelly, R.P., Feneley, M.P.: Relations between left atrial appendage blood flow velocity, spontaneous echocardiographic contrast and thromboembolic risk in vivo. J. Am. Coll. Cardiol. **23**(4), 961–969 (1994)
4. Lee, J.M., et al.: Why is left atrial appendage morphology related to strokes? An analysis of the flow velocity and orifice size of the left atrial appendage. J. Cardiovasc. Electrophysiol. **26**(9), 922–927 (2015)
5. Beigel, R., Wunderlich, N.C., Ho, S.Y., Arsanjani, R., Siegel, R.J.: The left atrial appendage: anatomy, function, and noninvasive evaluation. JACC Cardiovasc. Imaging **7**(12), 1251–1265 (2014)
6. Di Biase, L., et al.: Does the left atrial appendage morphology correlate with the risk of stroke in patients with atrial fibrillation? Results from a multicenter study. J. Am. Coll. Cardiol. **60**(6), 531–538 (2012)
7. Wootton, D.M., Ku, D.N.: Fluid mechanics of vascular systems, diseases, and thrombosis. Annu. Rev. Biomed. Eng. **1**(1), 299–329 (1999)
8. Nedios, S., et al.: Left atrial appendage morphology and thromboembolic risk after catheter ablation for atrial fibrillation. Heart Rhythm **11**(12), 2239–2246 (2014)
9. Otani, T., Al-Issa, A., Pourmorteza, A., McVeigh, E.R., Wada, S., Ashikaga, H.: A computational framework for personalized blood flow analysis in the human left atrium. Ann. Biomed. Eng. **44**(11), 3284–3294 (2016)
10. Guadalupe, G.I., et al.: Sensitivity analysis of geometrical parameters to study haemodynamics and thrombus formation in the left atrial appendage. Int. J. Numer. Method Biomed. Eng. **34**(8), 122–140 (2018)
11. Olivares, A.L., et al.: In silico analysis of haemodynamics in patient-specific left atria with different appendage morphologies. In: Pop, M., Wright, G.A. (eds.) FIMH 2017. LNCS, vol. 10263, pp. 412–420. Springer, Cham (2017). https://doi.org/10.1007/978-3-319-59448-4_39
12. Fernandez-Perez, G.C., Duarte, R., la de Calle, M.C., Calatayud, J., Sanchez Gonzalez, J.: Analysis of left ventricular diastolic function using magnetic resonance imaging. Radiologia **54**(4), 295–305 (2012)
13. Meng, H., Tutino, V.M., Xiang, J., Siddiqui, A.: High WSS or Low WSS? Complex interactions of hemodynamics with intracranial aneurysm initiation, growth, and rupture: toward a unifying hypothesis. Am. J. Neuroradiol. **35**(7), 1254–1262 (2014)
14. Di Achille, P., Tellides, G., Figueroa, C.A., Humphrey, J.D.: A haemodynamic predictor of intraluminal thrombus formation in abdominal aortic aneurysms. Proc. R. Soc. A Math. Phys. Eng. Sci. **470**(2172) (2014). https://doi.org/10.1098/rspa.2014.0163
15. Gautam, S., John, R.M.: Interatrial electrical dissociation after catheter-based ablation for atrial fibrillation and flutter. Circ. Arrhythmia Electrophysiol. **4**(4), 26–29 (2011)
16. Yamamoto, M., et al.: Complex left atrial appendage morphology and left atrial appendage thrombus formation in patients with atrial fibrillation. Circ. Cardiovasc. Imaging **7**(2), 337–343 (2014)
17. Khurram, I.M., et al.: Relationship between left atrial appendage morphology and stroke in patients with atrial fibrillation. Heart Rhythm **10**(12), 1843–1849 (2013)